Microelectronic Engineering 98 (2012) 301–304

Contents lists available at SciVerse ScienceDirect

Microelectronic Engineering

journal homepage: www.elsevier.com/locate/mee

Atomic resolution top-down nanofabrication with low-current focused-ion-beam thinning

Wuxia Li [a,b,*], Ajuan Cui [a], Changzhi Gu [a], P.A. Warburton [b]

[a] *Beijing National Lab of Condensed Matter Physics, Institute of Physics, Chinese Academy of Sciences, Beijing 100190, China*
[b] *London Centre for Nanotechnology, University College London, 17-19 Gordon Street, London WC1H 0AH, United Kingdom*

ARTICLE INFO

Article history:
Available online 3 August 2012

Keywords:
Size reduction
Atomic resolution
Focused-ion-beam
Thinning
Superconductivity

ABSTRACT

Techniques for scalable fabrication of one-dimensional or quasi-one-dimensional nanowires are of great importance to observe quantum size effects and build quantum information devices. In this work, we developed a technique for size reduction of both lateral and freestanding tungsten composite nanostructures using focused-ion-beam (FIB) thinning. Different exposure times and ion-beam currents were used to control the final size and the thinning rate and accuracy of a group of nanowires, an individual nanowire and a portion of a nanowire by low-current site-specific milling. A transmission electron microscope image of a thinned superconducting tungsten composite nanowire with width reduced from 80 nm to 50 nm shows uniform shrinking along the length of the wire and high resolution image shows no obvious changes of the morphology after thinning. The variation of the superconducting critical current density upon thinning is insignificant; it is 1.7×10^5 and 1.4×10^5 A/cm^2 at 4.26 K for the as-deposited and wire with width reduced to 50 nm, respectively. These results suggest that FIB-milling is a potential approach for controllable size reduction enabling the observation of size- and quantum effects.

1. Introduction

It has been demonstrated that when the diameter of a superconducting nanowire is reduced smaller than the Ginsburg–Landau phase coherence length and the magnetic penetration depth, below or near the superconducting transition temperature, the resistance of a 1D wire is no longer zero [1]. In principle, a wire can fall into one of the following three different categories: (i) truly superconducting, that is approaching zero resistance in the limit of zero temperature; (ii) resistive or normal with non-zero resistance even at zero temperature; and (iii) insulating, with resistance infinitely large when the temperature approaches zero. Intuitively, it is reasonable to expect thin wires to lose their superconducting qualities as the diameter is gradually reduced. Meanwhile, free-standing nanostructures are the fundamental building blocks of three-dimensional (3D) nanodevices with multi-functionality beyond that achievable by planar devices. For instance, a 3D superconducting quantum interference device (SQUID), formed by integrating a conventional SQUID with free-space multiple pick-up loops, potentially could overcome the present planar SQUID limitation of only being able to detect the field perpendicular to the substrate; however, to realize single spin detection resolution, the size of the 3D superconducting pick-up loop must be sub-micron, necessitating nanoscale superconducting wires [2].

Various fabrication technologies for nanometer scale features have been developed [3–10]. Among them, a combination of e-beam lithography, metal evaporation and lift-off process has been widely used to top down fabricate under 20 nm metal track (wires) in large scale [7]. However, nanowires based on materials that cannot be grown by deposition and lift-off techniques are unachievable by this method. For example, for the iron-based superconductor, $Cs_{0.8}(FeSe_{0.98})_2$ (grown at temperatures over 1000 °C, in the shape of well-formed black crystal rods a few mm in diameter [11]), an alternative direct and site-specific milling approach is required in order to study its superconductivity and the related size effect. FIB milling is a technique that can meet this requirement. It has attracted remarkable interest in recent years [8–10]. By FIB-milling, regular wide tracks or irregular micro- and nano-features can be thinned [10]. The advantages of FIB-milling include that it is a maskless and resistless process, applicable to most materials in any form (i.e. films, tracks, wires, particles and flakes).

In addition it has been reported that vertical tungsten nanowires grown by FIB-induced deposition are superconducting with much enhanced superconductivity [12–14], and could be used to form 3D nano-SQUIDs that potentially are able to detect the magnetic field both parallel and perpendicular to the substrate surface [2]. However, the size of the as-deposited 3D structures must be reduced if single-spin resolution and sensitivity are to be achieved. Thus is it of great importance to explore a reliable technique for

---

* Corresponding author at: Beijing National Lab of Condensed Matter Physics, Institute of Physics, Chinese Academy of Sciences, Beijing 100190, China. Tel.: +86 10 82649098; fax: +86 10 82648198.
E-mail address: liwuxia@aphy.iphy.ac.cn (W. Li).

0167-9317/$ - see front matter © 2012 Elsevier B.V. All rights reserved.
http://dx.doi.org/10.1016/j.mee.2012.07.108

fabricating nanometer-scale freestanding superconducting nanostructures, for better understanding of superconductivity at nanometer scale as well as towards the realization of high-performance 3D superconducting nanodevices.

In this work, we demonstrate that by FIB milling, the size of a nanowire can be effectively reduced. In detail, freestanding tungsten nanowires were grown on SiO_2/Si by FIB-CVD using a 1 pA ion-beam current; then nanowires were felled by FIB milling followed by low current FIB thinning to reduce the size locally. Different exposure times and ion-beam currents were used to control the final size and the thinning rate and accuracy. Microscopy analysis indicates no significant changes of the morphology and microstructure. Temperature dependent electrical measurements shows that the superconducting critical current density at 4.26 K for the as-deposited nanowire is about 1.7×10^5 A/cm^2 and that of the wire with width reduced to 50 nm is 1.4×10^5 A/cm^2. Additionally a 200 pA ion beam current was used to irradiate vertically grown nanowires by reduced-raster scanning to form electrical contacts as well as to reduce the size of the freestanding wires simultaneously. Our results suggest that FIB-thinning is a potential approach for controllable size reduction with high resolution towards the observation of size- and quantum effects.

2. Experimental details

The tungsten nanowires were grown using FIB-CVD. A commercially available FIB system utilizing a beam of 30 keV singly-charged Ga^+ ions was used for all the experiments conducted in this study. Gaseous tungsten hexacarbonyl ($W(CO)_6$) was injected in the vicinity of the focused beam scanned area through a nozzle. The vertically grown nanowires were then felled by lateral FIB milling through the base of the nanowires. Then the size of the nanowire was thinned by raster or/and reduced raster scanning with various ion beam exposure durations, to reduce the size of the whole wire evenly or a portion of it. The width, thickness and height of nanowires were measured by *in situ* SEM and by atomic force microscope (AFM). After thinning, nanowires were transferred onto holey carbon TEM grids by an *in situ* nano-manipulator. The chemical composition was obtained by energy dispersive X-ray spectroscopy (EDS) and electron-energy loss spectroscopy attached to the TEM.

To form a four-terminal device configuration for electrical properties measurement, a larger ion beam current of 10 pA was then used to deposit strips to connect the thinned wire to large Au contact pads, which had been previously formed on a 200-nm-thick SiO_2 layer on a Si substrate by conventional photolithography-based processes. Current-biased transport measurements were performed with a Quantum Design Physics Properties Measurement System (PPMS).

In order to develop a technology for thinning of freestanding nanowires, we systematically investigated the optimized condition for FIB-milling size reduction as well as the general bending effect, including the influence of the ion beam current and the ion incident-angle during thinning, which has been reported elsewhere [15]. To thin a pair of vertical nanowires as well as to obtain a solid contact between them, a reduced-raster scan was performed so that the beam scanned in an area that covered the wire to be bent and a portion of the other wire with an ion beam current in the range 150–300 pA. The stage rotation and tilting angles were also optimized based on the values of the interspacing and heights of wires to be bent.

3. Results and discussion

Fig. 1(a) shows a typical SEM side view image of a vertical tungsten nanowire deposited using a 1 pA ion beam current; the diameter of the wire is about 80 nm. Fig. 1(b) is the plan-view image of the wire being thinned using reduced raster scanning with a 1 pA ion beam. The segment indicated by number 3 is the as-deposited portion. The tapered shape was formed by ion-beam irradiation in an area sufficient to cover segments 1 and 2 together for 4 min, followed by another 2 min on segment 1 alone. The horizontal field width was 16.2 μm. Using a reduced raster scan, the total scanning area was set to be 4 μm in width. It can be seen that the width of the wire was reduced from 80 nm to 50 and then to 20 nm. A milling rate of approximately 0.60 μm^3/nC can be derived accordingly. For accurate control of the size reduction, it is necessary to use a low ion-beam current and low magnification. An increased size reduction rate can be obtained with larger ion-beam currents and magnifications, though this sacrifices controllability. A high milling rate may also damage the supporting substrate. To obtain a nanowire with evenly-reduced size along the length direction, raster scanning with a field of view that barely covers the nanowire was used to avoid unnecessarily harsh thinning.

Fig. 2 shows the transmission electron microscope image of a thinned tungsten nanowire promptly inserted into a TEM facility for structural properties examination. The bright field image in Fig. 2(a) shows that the width was reduced to about 50 nm. An image at a higher magnification is shown in Fig. 2(b), confirming that the thinned nanowires do not display any long-range crystalline order – rather there are nanocrystallites with grain size on the order of 1 nm, a result similar to those observed for the as-deposited nanowire [12]. This further indicates that low-current ion-beam milling did not bring observable change to the microstructure of the tungsten nanowires. However, the outer amorphous layer is slightly thinner compared to the as-deposited nanowire (not shown here), confirming the removal of the outer amorphous layer during thinning. The Electron-energy loss and energy dispersive X-ray spectroscopy show that the composition of the thinned nanowire is 49 at.% tungsten, 29 at.% carbon, 16 at.% gallium and 6 at.% oxygen. This composition is similar to that reported previously [13], indicating that FIB thinning of the as-deposited objects leads to no obvious changes in their chemical composition.

Temperature-dependent resistance and I–V transport measurements were conducted on the as-deposited nanowire and that with width thinned to 50 nm. Fig. 3 shows the I–V curves. In the inset of

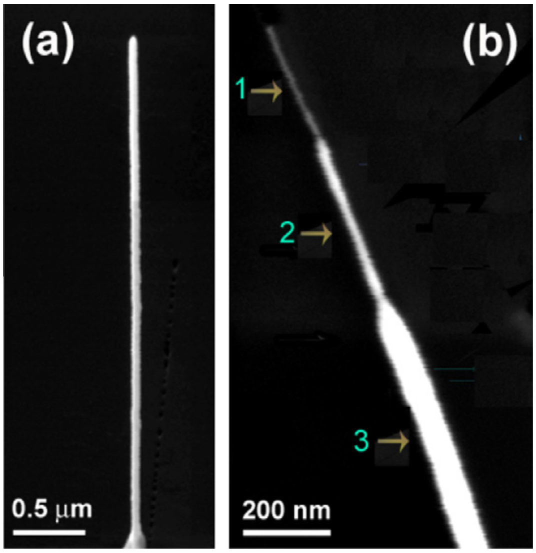

Fig. 1. (a) SEM side view image of a freestanding tungsten nanowire grown by FIB-induced deposition and (b) SEM top view image of a tapered tungsten nanowire thinned by FIB after being felled by FIB at the base. The nanowire growth, felling and thinning were conducted with a 1 pA ion beam.

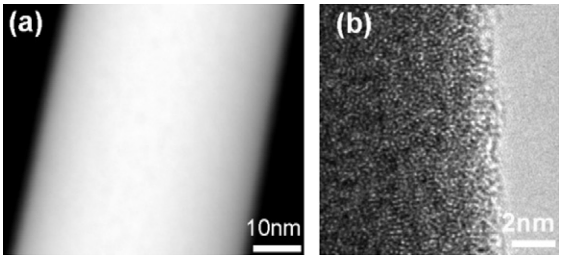

Fig. 2. (a) Transmission electron microscope (TEM) image of a tungsten nanowire with width reduced to 50 nm and (b) high resolution TEM image of the wire at its edge.

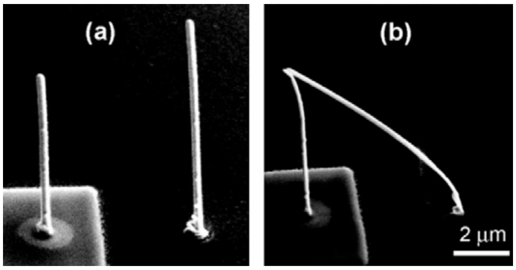

Fig. 4. (a) SEM image of the as-grown vertical tungsten nanowires (330 nm in width) and (b) nanowires bent to form air-bridge structure with width halved by the irradiation using a 200 pA ion beam during the bending process.

Fig. 3 is a typical four-terminal configuration formed on a thinned tungsten nanowire. Both the as-deposited and thinned nanowires show superconducting transitions above 5.0 K; here T_c is defined as the temperature at which the resistivity falls to 50% of its value at the onset of the transition. The transition width of the 50 nm wide nanowire is slightly wider than that of the as-deposited one (80 nm). This observation is consistent with the previous report [14] that for FIB-grown tungsten wires the width of the transition increases for wires of diameter below 60 nm.From the I–V curves, it can be derived that the critical current density upon thinning is insignificant, being 1.7×10^5 and 1.4×10^5 A/cm^2 at 4.26 K for the as-deposited and wire with width reduced to 50 nm, respectively. In our previous study, it has been found that for as-deposited lateral nanowires with width 19 nm, a residual resistive tail extending down to the low-temperature region exists, possibly as a consequence of a thermally activated phase slip (TAPS) process near T_c [16,17]. However, the coherence length of FIB deposited tungsten is about 6 nm. Using most of the currently available commercial FIB systems, it is still a technical challenge to deposit freestanding nanowires with diameter less than 80 nm, and to deposit lateral continuous thin nanowires with width and/or thickness less than 10 nm. So the approach of using low-current FIB thinning to reduce the size of the as-deposited nanofeature to the physical critical values might find potential application in the research fields of quantum science as well as nanoscience and nanotechnology.

To demonstrate the applicability of this technique to the thinning of freestanding nanowires, two vertically grown tungsten nanowires with heights of 7.8 and 5.5 μm, spaced by 5.5 μm were used. Fig. 4 shows the joint contact formed between these two wires with the width having been halved by using a 200 pA ion-beam current. To achieve such structures, the stage was rotated by 80° so that the two wires were slightly misaligned, then reduced raster scanning was performed to irradiate the whole of the longer wire and a small section of the shorter wire as shown in Fig. 4. Here the stage was tilted by 45°, so that the longer wire bent towards the incident ion beam and finally made contact with the shorter one. Both wires were thinned by the ion beam scanning process. This confirms that FIB milling can be used for controllable size reduction as well as to manipulate the orientation of freestanding nanowires at the same time. We expect to conduct further experiment to integrate such structure with a planar SQUID for super-performance 3D nano-SQUID fabrication in the near future.

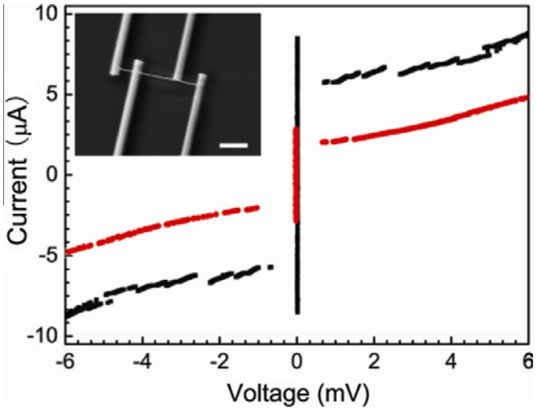

Fig. 3. I–V characteristics of the as-deposited wire with width of 80 nm (black curve) and a thinned nanowire with width of 50 nm (red curve) measured at 4.26 K. In the inset is the SEM image of a four terminal configuration formed on a tungsten nanowire with width reduced to 25 nm. (For interpretation of the references to colour in this figure legend, the reader is referred to the web version of this article.)

4. Conclusion

In summary, we have developed a technique for site-specific nanowire size reduction by FIB thinning. Transmission electron microscope images of a thinned tungsten composite nanowire with width reduced from 80 to 20 nm show uniform shrinking along the length of the wire and high resolution images show no obvious changes of the morphology after thinning. The critical current density of the as-deposited wire and one thinned to a width of 50 nm is 1.7×10^5 and 1.4×10^5 A/cm^2 at 4.26 K, respectively, suggesting insignificant modulation of the electrical properties during thinning. These results suggest that FIB-milling is a potential approach for controllable size reduction with high resolution towards the observation of size- and quantum effects, as well as for construction of 3D superconducting nanodevices.

Acknowledgments

This work is supported by the National Natural Science Foundation of China under Grants Nos. 91123004, 11104334, 50825206, 10834012, and 60801043; by the Outstanding Technical Talent Program of the Chinese Academy of Sciences; by Chinese Service Center for Scholar Exchange; by the National Basic Research Program (973) of China under Grant No. 2009CB930502; by the IRC in Nanotechnology; and by EPSRC contract EP/F035411/1.

References

[1] A. Bezryadin, J. Phys. Condens. Matter 20 (2008) 043202.
[2] E.J. Romans, E.J. Osley, L. Young, P.A. Warburton, W. Li, Appl. Phys. Lett. 97 (2010) 222506.
[3] C.R. Martin, Science 266 (1994) 1961.
[4] V.Y. Butko, J.F. Ditusa, P.W. Adams, Phys. Rev. Lett. 84 (2000) 1543.
[5] G. Abadal, F. Perez-Murano, N. Barniol, X. Aymerich, Appl. Phys. A 66 (1998) S791.
[6] A. Bezryadin, C.N. Lau, M. Tinkham, Nature 404 (2000) 971.
[7] M. Zgirski, K.Y. Arutyunov, Phys. Rev. B 75 (2007) 172509.
[8] H.H. Cheng, M.M. Alkaisi, S.E. Wu, C.P. Liu, AIP Conf. Proc. 1151 (2009) 48.
[9] A.P.G. Troeman, H. Derking, B. Borger, J. Pleikies, D. Veldhius, H. Hilgenkamp, Nano Lett. 7 (2007) 2152.

[10] G.C. Tettamanzi, C.I. Pakes, S.K.H. Lam, S. Prawer, Supercond. Sci. Techno. 22 (2009) 064006.
[11] A. Krzton-Maziopa, Z. Shermadini, E. Pomjakushina, V. Pomjakushin, M. Bendele, A. Amato, R. Khasanov, H. Luetkens, K. Conder, J. Phys. Condens. Matter 23 (2011) 052203.
[12] W. Li, C.Z. Gu, P.A. Warburton, J. Nanosci. Nanotechnol. 10 (2010) 7436.
[13] W. Li, J.C. Fenton, P.A. Warburton, IEEE Trans. Appl. Supercond. 19 (2009) 2819.
[14] W. Li, J.C. Fenton, C.Z. Gu, P.A. Warburton, Microelectron. Eng. 88 (2011) 2636.
[15] W. Li, J.C. Fenton, Nanotechnology 23 (2012) 105301.
[16] A. Rogachev, A. Bezryadin, Appl. Phys. Lett. 83 (2003) 512.
[17] N. Lau, N. Markovic, M. Bockrath, A. Bezryadin, M. Tinkham, Phys. Rev. Lett. 87 (2001) 217003.